Smart Energy and Sustainable Environment

2020, *23*(1): 35-46, https://doi.org/10.46390/j.smensuen.23120.80

HYDROCHEMICAL CHARACTERIZATION AND QUALITY OF SURFACE WATER FROM OLT RIVER, ROMANIA

Claudia Sandru*, Mihaela Iordache, Andreea Maria Radulescu, Ramona Ionela Zgavarogea, Roxana Elena Ionete

National Research and Development Institute for Cryogenics and Isotopic Technologies – ICSI Rm. Valcea, 4th Uzinei Street, P.O. Box Râureni 7, 240050, Rm. Valcea, Romania

Abstract:

Hydrochemical investigations of the surface water and the seasonal effect on the chemical budget of ions from the Olt river were carried out. Geochemical results show that the seasonal effect does not change the order of ion abundance. The Piper diagram was used for the classification of cations and anions, in terms of confidence in the major percentages of ions and types of water. According to the Piper diagram, the dominant hydrochemical facies in the study area is Ca–Na–HCO_3^-–Cl^-, which represents 87% of the samples. The study area is influenced by natural processes of water–rock interaction such as dissolution of evaporitic rocks (gypsum, anhydrite, and halite).

Article info:

Received 03 February 2020
Received in revised form 20 February 2020
Accepted 27 February 2020
Available online 06 March 2020

Keywords*:*
geochemistry, water quality, surface water

How to cite: Sandru, C., Iordache, M., Radulescu, A. M., Zgavarogea, R. I. Ionete, R. E., (2020). Hydrochemical characterization and quality of surface water from Olt river, Romania. *Smart Energy and Sustainable Environment, 23*(1), 35-46.

1. INTRODUCTION

Knowledge of the water hydrochemistry is an essential element when the origin of its chemical composition has to be determined (Zaporozec, 1972). Therefore, detailed studies have been performed during the years in many parts of the globe. Chemical substances transported by rivers have been studied using geochemical budgets for more than one hundred years (Forel, 1892). The most abundant materials dissolved in rivers are ions that originate from terrestrial and atmospheric systems, which are mainly calcium (Ca^{2+}), magnesium (Mg^{2+}), sodium (Na^+), potassium (K^+), bicarbonate (HCO_3^-), sulfate (SO_4^{2-}), chloride (Cl^-) and nitrate (NO_3^-) (Meybeck and Ragu, 1995). The ionic chemistry of rivers can provide essential information about both the processes affecting the continental surface (e.g. rock weathering, atmospheric precipitation, evaporation-crystallization) and the amount of natural material carried by river water bodies (Gibbs, 1970; Meybeck, 1982).

*Corresponding author: Claudia Sandru, e-mail: claudia.sandru@icsi.ro, ORCID: 0000-0002-5168-7290

In this work, a hydrochemical investigation of the surface water of the Olt River, Romania, an important tributary of the Danube, is performed, together with the influence of seasonal effect on the chemical budget of ions from the river waters, to better assess the impact of anthropic activities and industry/agriculture. This study aim to provide useful information for the management and a sustainable development of the Olt River.

2. MATERIALS AND METHODS

2.1. Study area

The investigation area was set on the Olt River (Romania) that flows into the Danube River near Turnu Magurele, at Islaz, and has a total length of 615 km. The middle and lower part of the Olt River catchment includes 19 lakes used for generating electricity/power and for agricultural practices (irrigation systems). The average flow of the Olt River is 140 $m^3 \cdot s^{-1}$ with monthly variations from 25 to 300 $m^3 \cdot s^{-1}$. The largest amount of the annual flow volume of the Olt takes place in May when the snows melts in the mountains and there are abundant spring rains; it often exceeds several times the average annual flow. Maximum recorded at Ramnicu Valcea reached 2580 $m^3 \cdot s^{-1}$. The lowest flows are registered in September and October after the period of minimum precipitation and evaporation in August and September and strong before winter maximum rainfall event.

The water samples subject to this study were collected in 22 locations (Table 1), including 19 accumulation lakes, 1 point from the Olt River before flowing into the Danube River and 2 points in the Danube River (upstream and downstream of the Olt River), during two seasons (spring and summer).

Table 1. Water/sediment sampling points

Code	Coordinates/Sampling location, County	Code	Coordinates/Sampling location, County
A1	N: 45°24’337; E: 24°18’255 Cornet accumulation lake, Valcea	A12	N: 43°42’693; E: 24°46’610 Danube River – upstream the Olt River, Teleorman
A 2	N: 45°21’312; E: 24°16’350 Lotru accumulation lake, Valcea	A13	N: 43°44’630; E: 24°46’777 Olt River - Islaz, before flowing into the Danube River, Teleorman
A3	N: 45°17’200; E: 24°18’365 Turnu accumulation lake, Valcea	A14	N: 43°42’792; E: 24°53’463 Danube River– downstream the Olt River, Teleorman
A4	N: 45°14’522; E: 24°20’855 Calimanesti accumulation lake, Valcea	A15	N: 43°48’682; E: 24°42’318 Izbiceni accumulation lake, Olt
A5	N: 45°10’723; E: 24°22’200 Daesti lake accumulation, Valcea	A16	N: 43°54’772; E: 24°37’680 Rusanesti accumulation lake, Olt
A6	N: 45°07’510; E: 24°22’382 Ramnicu Valcea accumulation lake, Valcea	A17	N: 43°54’988; E: 24°37’463 Frunzaru accumulation lake, Olt
A7	N: 45°00’542; E: 24°17’922 Govora accumulation lake, Valcea	A18	N: 44°09’468; E: 24°28’415 Draganesti accumulation lake, Olt
A8	N: 44°55’030; E: 24°14’983 Babeni accumulation lake, Valcea	A19	N: 44°15’517; E: 24°37’680 Ipotesti accumulation lake, Olt
A9	N: 44°51’468; E: 24°16’927 Ionesti accumulation lake, Valcea	A20	N: 44°25’322; E: 24°20’738 Slatina accumulation lake, Olt
A10	N: 44°46’620; E: 24°16’935 Zavideni accumulation lake, Valcea	A21	N: 44°26’877; E: 24°19’087 Arcesti accumulation lake, Olt
A11	N: 44°07’790; E: 24°17’888 Dragasani accumulation lake, Valcea	A22	N:44°32’762; E: 24°20’370 Strejesti accumulation lake, Olt

2.2. Sample Collection and Pre-treatment

Sampling campaign was organized in 2018, from March to June 2018, covering 22 locations across the river. Standard methods were used for collecting and analyzing the water samples (SR EN ISO 5667-6, 2017). Water sampling was made in clean glass bottles, prior rinsed with deionized water and stored to the laboratory for up to 24 h, at 4°C, to retard the microbiological activity as well as the rates of possible physical and chemical reactions.

2.3. Analytical procedure

The analytical methods used in environmental monitoring have greatly evolved. For unstable parameters such as electrical conductivity (EC) and pH, the measurement was performed at the sampling site. Samples were taken to the laboratory for analysis of physico-chemical parameters like calcium, magnesium, sodium, chlorides, sulphates, nitrates, bicarbonates, and total dissolved solids (TDS).

The nitrate and sulphate concentrations in samples were determined by colorimetric method, using a UV-VIS spectrophotometer type SPECORD 250. All the results, for nitrate and sulphate concentration are expressed in $mg \cdot L^{-1}$. Chloride ions were generally determined by titrating the water samples against a standard solution of $AgNO_3$ using potassium chromate as an indicator. The bicarbonate alkalinity of the water samples was determined by titration with hydrochloric acid. For pH measurement the electrochemical method was used, while for total dissolved solids the gravimetric method. According to standard methods, the Ca^{2+}, Mg^{2+}, and Na^{+} content was determined by flame atomic absorption spectroscopy (AAS). Thus, an AAS NOVAA 300 model, with Air-C_2H_2 flame type of an average fuel flow rate between 0.8-4.0 $L \cdot min^{-1}$ and the carrier gas flow rate between 13.5-17.5 $L \cdot min^{-1}$, was used for water samples analysis. Hallow cathode lamps of the different metals were used as radiation sources and the analytical measurements based on time-averaged absorbance. Resonance lines at 422.7, 285.2, and 589.0 nm were employed for Ca, Mg, and Na. Lamp intensity (4-6 mA) and band pass (0.2-0.5 nm) were used. Air/acetylene flow rates were between 0.9-1.1 $L \cdot min^{-1}$ for all metals. Prior to each series of measurements, a calibration line was created for each element.

Reagents used during the study were of spectroscopic grade; the multielement standard solution CertiPur® with a certified value of 1000 ± 3 $mg \cdot L^{-1}$ from Merck (Germany) was used for the calibration curve in the quantitative analysis. Ultrapure water with a maximum resistivity of 18.2 $M\Omega \cdot cm^{-1}$, was used for sample treatment and dilution. The working standards and control sample were prepared daily from the intermediate standards that were earlier prepared from the stock solutions. Each determination was carried out twice and the range and median values were reported. All the investigated calibration curves were characterized by a high correlation coefficient ($r > 0.995$) for both analytical methods.

3. RESULTS AND DISCUSSION

3.1. General hydrogeochemistry

The ionic composition of the Olt River water is presented as box plot in Fig.1 and detailed per location in Table 2. The pattern of cationic dominance based on mean values ($mg \cdot L^{-1}$) in the Olt River are in the following order: $Ca^{2+} > Na^{+} > Mg^{2+}$. The results

exhibited that out of the total cationic-budget in the Olt River water, Ca^{2+} alone contributes 63.41%, Na^{+} with 31.03% and Mg^{2+} account for 5.56%.

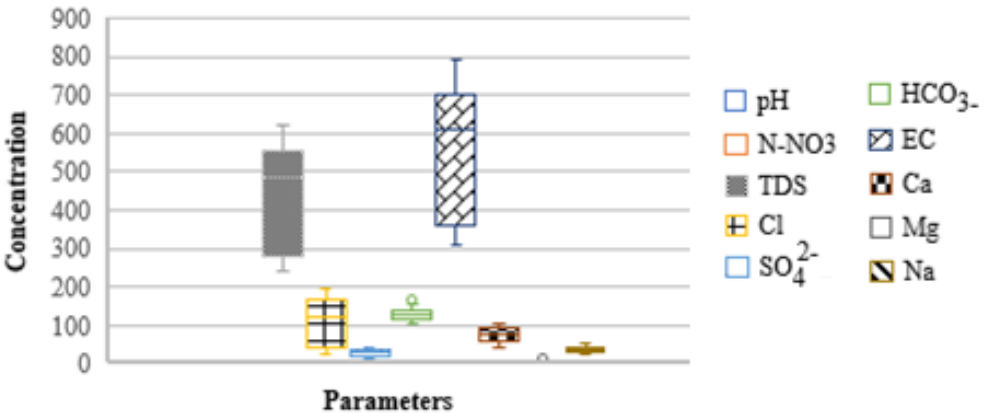

Figure 1. Box plot for the maximum, minimum and average of the chemical constituents (*all values in mg/L except conductivity (µS·cm^{-1}) and pH*)

Table 2. Summary statistics of hydrochemical composition of the Olt River (mean values, standard deviation and domain of variation) by locations (sampling points)

Location		pH	NO_3^-	TDS	Cl^-	SO_4^{2-}	HCO_3^-	EC	Ca^{2+}	Mg^{2+}	Na^+
A1	Mean	7.99	0.19	280.75	40.33	19.00	118.83	360.75	46.54	5.73	25.01
	Min.	7.67	0.16	208.00	22.68	14.00	30.00	283.00	29.43	3.42	12.76
	Max.	8.38	0.23	379.00	62.39	22.00	189.10	480.00	59.94	7.54	37.88
	SD	0.36	0.03	71.39	20.35	3.56	65.83	83.98	12.82	1.74	10.47
A2	Mean	7.89	0.20	278.25	31.11	15.25	141.85	357.25	47.03	5.58	27.62
	Min.	7.30	0.14	211.00	20.56	12.00	116.00	288.00	33.69	3.48	14.02
	Max.	8.40	0.27	375.00	52.11	19.00	183.00	475.00	61.93	7.23	48.28
	SD	0.56	0.06	69.23	14.46	3.30	28.74	81.52	11.80	1.65	14.92
A3	Mean	8.05	0.17	243.00	24.70	20.00	117.48	308.75	42.25	5.26	23.31
	Min.	7.71	0.13	207.00	18.43	16.00	109.80	267.00	29.45	3.49	11.74
	Max.	8.37	0.20	262.00	35.00	23.00	128.10	332.00	48.67	6.45	32.61
	SD	0.34	0.03	25.26	7.72	3.16	7.66	29.75	8.86	1.26	8.80
A4	Mean	7.94	0.20	265.75	26.17	18.25	114.38	336.00	45.26	5.49	23.12
	Min.	7.63	0.13	216.00	15.59	17.00	85.40	273.00	30.70	3.54	12.64
	Max.	8.36	0.31	359.00	40.20	19.00	164.70	455.00	56.80	6.42	32.09
	SD	0.32	0.08	65.42	11.37	0.96	37.73	83.77	10.92	1.35	8.37
A5	Mean	8.00	0.13	279.25	29.18	18.00	132.73	354.75	62.37	5.47	24.80
	Min.	7.67	0.10	232.00	9.92	16.00	116.00	303.00	30.67	3.73	14.16
	Max.	8.30	0.17	385.00	53.60	21.00	170.80	483.00	106.70	7.16	37.99
	SD	0.34	0.03	71.01	18.47	2.45	26.02	85.75	32.69	1.46	10.35
A6	Mean	8.14	0.15	250.50	34.96	20.75	126.58	315.00	57.10	5.07	29.41
	Min.	7.76	0.13	232.00	14.18	15.00	122.00	291.00	29.34	3.75	14.21
	Max.	8.50	0.17	283.00	58.30	26.00	140.30	359.00	107.10	5.68	54.05
	SD	0.32	0.02	23.16	19.07	4.57	9.15	31.62	34.28	0.91	17.64
A7	Mean	8.31	0.16	349.25	83.68	23.25	122.00	440.50	58.06	4.96	29.85
	Min.	7.75	0.07	229.00	19.85	20.00	97.60	283.00	30.55	3.45	12.97
	Max.	9.10	0.25	621.00	234.00	26.00	134.20	786.00	107.90	5.90	55.33
	SD	0.58	0.09	182.87	100.77	2.50	16.52	232.93	34.11	1.10	18.32

Location		pH	NO_3^-	TDS	Cl^-	SO_4^{2-}	HCO_3^-	EC	Ca^{2+}	Mg^{2+}	Na^+
A8	Mean	8.09	0.12	617.50	188.68	20.00	105.23	784.50	99.81	5.10	42.96
	Min.	7.77	0.07	340.00	55.30	11.00	91.50	442.00	42.84	3.91	23.59
	Max.	8.43	0.16	880.00	303.00	29.00	134.20	1114.00	148.50	6.27	59.03
	SD	0.33	0.04	220.64	106.16	8.83	20.15	274.46	43.55	0.97	15.60
A9	Mean	8.01	0.11	623.75	191.70	23.25	125.05	791.00	102.83	5.10	43.47
	Min.	7.75	0.07	356.00	66.65	11.00	109.80	455.00	43.61	3.93	23.99
	Max.	8.37	0.15	878.00	296.00	33.00	134.20	1111.00	152.40	6.40	59.48
	SD	0.26	0.04	213.28	96.80	10.97	11.68	268.01	45.15	1.02	15.52
A10	Mean	8.00	0.10	616.50	194.45	30.00	102.18	779.75	102.31	5.25	43.36
	Min.	7.66	0.06	339.00	63.81	16.00	91.50	427.00	39.02	4.26	23.78
	Max.	8.43	0.16	881.00	312.70	44.00	109.80	1115.00	156.20	6.33	59.67
	SD	0.34	0.05	221.40	103.23	13.17	9.15	281.07	48.36	0.90	15.88
A11	Mean	8.05	0.04	578.75	173.00	31.25	123.53	733.00	93.62	5.69	41.28
	Min.	7.63	0.02	449.00	83.66	19.00	122.00	575.00	57.61	5.19	27.03
	Max.	8.60	0.07	697.00	233.90	42.00	128.10	881.00	116.70	6.21	52.43
	SD	0.41	0.03	107.50	70.28	11.47	3.05	133.44	25.28	0.54	12.54
A12	Mean	7.85	0.07	360.50	42.92	28.50	155.55	454.50	73.49	13.28	28.51
	Min.	7.80	0.01	328.00	31.30	22.00	122.00	411.00	52.60	5.36	20.13
	Max.	7.97	0.13	388.00	66.65	37.00	195.20	490.00	101.20	21.14	51.37
	SD	0.08	0.07	30.51	16.08	6.56	39.06	40.04	20.92	6.46	15.27
A13	Mean	7.91	0.07	494.50	126.79	40.00	146.40	626.00	90.02	9.68	39.42
	Min.	7.20	0.01	420.00	93.10	34.00	134.20	531.00	82.45	5.57	29.69
	Max.	8.20	0.13	612.00	158.80	46.00	170.80	774.00	101.10	14.32	54.65
	SD	0.48	0.07	84.52	33.98	5.16	16.52	106.76	8.41	3.65	11.15
A14	Mean	8.14	0.07	391.25	60.98	26.75	169.28	495.00	80.58	10.55	34.69
	Min.	8.00	0.01	338.00	29.80	19.00	152.50	427.00	68.82	5.21	19.19
	Max.	8.40	0.12	510.00	103.52	39.00	219.60	646.00	101.70	14.72	54.27
	SD	0.18	0.06	79.84	30.89	9.03	33.55	101.58	14.78	3.99	15.59
A15	Mean	8.25	0.11	485.50	118.31	36.75	128.10	613.50	73.91	7.15	39.82
	Min.	7.80	0.02	390.00	93.60	31.00	103.70	493.00	46.41	5.17	25.13
	Max.	8.49	0.17	613.00	156.00	44.00	158.60	772.00	91.48	9.10	54.64
	SD	0.31	0.06	94.69	30.05	5.62	28.61	118.47	19.35	1.68	13.70
A16	Mean	8.33	0.10	479.50	125.16	40.00	122.00	607.25	68.80	7.40	54.83
	Min.	8.30	0.02	393.00	95.00	36.00	109.80	497.00	45.98	5.51	26.36
	Max.	8.40	0.14	572.00	163.10	46.00	140.30	727.00	78.17	8.65	93.80
	SD	0.05	0.06	78.10	34.02	4.90	14.94	99.97	15.32	1.35	28.22
A17	Mean	8.33	0.11	488.75	120.44	43.25	131.20	619.00	75.00	7.28	53.59
	Min.	8.10	0.01	418.00	96.43	39.00	116.00	533.00	44.34	5.40	28.23
	Max.	8.50	0.16	557.00	174.40	48.00	152.50	706.00	87.50	9.28	88.84
	SD	0.21	0.07	67.18	36.23	3.69	18.24	83.48	20.50	1.75	25.77
A18	Mean	8.29	0.11	484.50	121.21	37.00	141.83	610.50	87.40	5.93	37.16
	Min.	8.00	0.01	417.00	100.50	32.00	134.20	519.00	74.52	5.17	30.67
	Max.	8.70	0.17	524.00	167.34	41.00	146.40	663.00	101.50	7.45	45.97
	SD	0.30	0.07	46.67	31.03	3.92	5.84	63.08	12.35	1.04	6.93
A19	Mean	8.24	0.06	510.50	133.67	35.00	125.90	584.75	78.59	5.71	49.37
	Min.	8.05	0.01	386.00	79.41	33.00	97.60	470.00	62.40	4.84	26.80
	Max.	8.40	0.10	598.00	177.27	38.00	170.80	758.00	99.50	6.54	88.43
	SD	0.19	0.04	95.22	46.85	2.16	34.18	134.51	18.04	0.73	29.08

Location		pH	NO_3^-	TDS	Cl^-	SO_4^{2-}	HCO_3^-	EC	Ca^{2+}	Mg^{2+}	Na^+
A20	Mean	8.59	0.10	498.50	130.69	38.00	106.75	630.25	88.68	7.41	37.82
	Min.	8.07	0.03	370.00	68.07	34.00	91.50	471.00	63.39	5.47	29.01
	Max.	8.89	0.16	581.00	171.60	42.00	140.30	730.00	103.50	9.62	50.83
	SD	0.36	0.07	97.50	48.67	3.37	22.55	120.84	18.58	2.15	10.55
A21	Mean	8.47	0.08	606.00	177.05	38.00	134.20	764.75	101.25	5.71	46.75
	Min.	7.73	0.01	593.00	140.40	30.00	122.00	749.00	88.80	4.86	39.80
	Max.	8.92	0.14	631.00	211.30	48.00	152.50	799.00	113.70	6.53	53.02
	SD	0.55	0.08	16.99	29.02	8.49	14.94	23.21	10.17	0.77	5.45
A22	Mean	8.58	0.19	548.25	162.86	38.25	114.38	692.00	90.86	7.15	38.88
	Min.	8.20	0.14	385.00	69.49	31.00	103.70	478.00	63.07	5.17	33.18
	Max.	8.70	0.32	622.00	214.14	42.00	122.00	788.00	107.70	9.10	44.70
	SD	0.25	0.09	109.69	63.86	5.19	9.15	143.73	20.81	1.68	5.43

All the values are in $mg \cdot L^{-1}$ except conductivity ($\mu S \cdot cm^{-1}$) and pH

The average anionic concentrations ($mg \cdot L^{-1}$) follow a pattern of dominance that is consistent with the previous results: $HCO_3^- > Cl^- > SO_4^{2-} > NO_3^-$. The dominant anion in the Olt River is HCO_3^- which accounts for 48.48%, followed by Cl^- and SO_4^{2-} with 40.40% and 11.07%, respectively. The NO_3^- was reported as the least abundant anion throughout the basin with an average contribution of 0.05%. The relatively high concentrations of bicarbonates, chlorides and sulphates indicating the contribution of rock weathering as well as evaporite dissolutions as the main processes that determine the hydrochemistry in the basin.

The pH carried from neutral to alkaline for all the sampling points. The highest pH (8.92) was noted from water samples of the Arcesti accumulation lake, (A21), while the lowest pH (7.20) of the Olt River-Islaz, before flowing into the Danube River, at location A13, in Teleorman county. The substantially elevated concentrations of EC and TDS were registered for the sampling points A7, A8, A10, A14, A15, A17, A19, A20, A21 and A22. This thing is most probably due to the excessive chemical weathering and physical erosion along with evaporation-crystallization processes.

The concentrations of Na and Cl^- are much higher in the sampling points A7÷A11 from Valcea County, in the sampling point A13 in Teleorman County, as well as from all the sampling points in county Olt, possibly due to the climatic and geological factors. The contrasting concentrations of the dissolved ions indicate how the climatic, hydrological and lithological differences can affect the hydrogeochemical processes in the river water.

3.2. Characterization of hydrogeochemical facies

Graphical representation of surface water major dissolved constituents (major cations and major anions) helps in understanding its hydrochemical evolution, grouping and areal distribution. River water is characterized by an atmospheric contact surface continuously moving and at an appreciable speed. The chemical composition of the surface water depends on the nature of the soils crossed by the watercourse, the soils in the receiving basin, but also the fact that it is charging with atmospheric gases (O_2, N_2, and CO_2) through its free surface. The term hydrochemical facies is used to describe the bodies of surface water in an aquifer that differs in their chemical composition. The facies are a function of the lithology, solution kinetics and flow patterns of the aquifer, and for our study this was highlighted in Figure 2, were the analytical data are represented by a Piper diagram.

The classification for cation and anion facies, in terms of major ion percentages and water types, is according to the domain in which they occur on the diagram segments. From

the cationic and anionic triangular fields of the Piper diagram, it is observed that 100% of water samples fall into the no dominant type; conversely, 27% of these water samples fall into the bicarbonate type and other 14% into the no dominant type and 59% into the chloride type in anion facies.

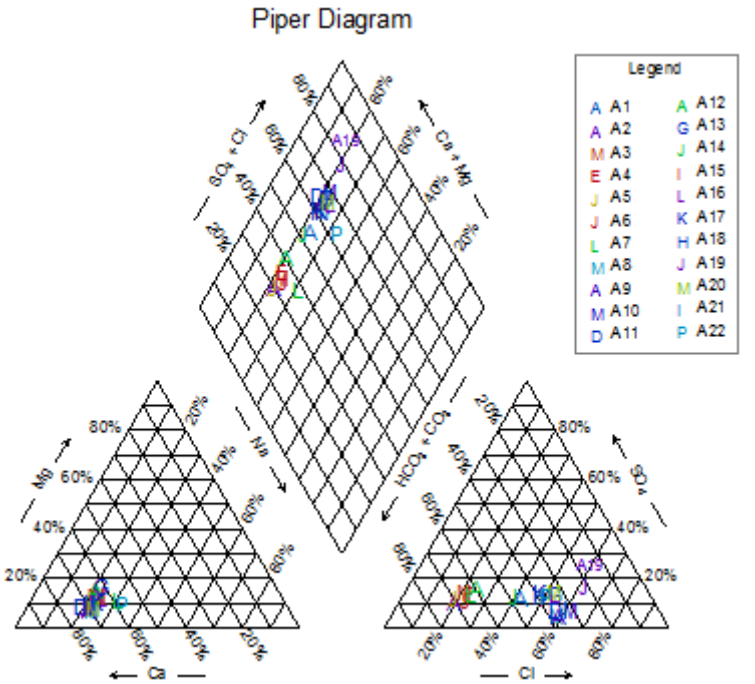

Figure 2. Piper diagram for describing the hydrochemical facies variation

The diamond shaped field between the two triangles is used to represent the composition of water with respect to both cations and anions. For both cations and anions the points are plotted on the appropriate triangle diagrams and their positions are projected parallel to the magnesium and sulphate axes, respectively, until they intersect in the center field. The plot of chemical data on diamond shaped trilinear diagram reveals that for majority of the surface water samples the metals alkaline exceeds metals alkaline earth. From the data plots (Fig. 2), it is apparent that the total hydrochemistry is dominated by metals alkaline.

3.3. Major sources and controlling factors of hydrogeochemistry

The mechanisms controlling the hydrogeochemistry (Table 3) of surface water can be inferred from the Gibbs schematic diagram:

a) low TDS (<10 $mg \cdot L^{-1}$) concentrations and high ratios of Na/(Na+Ca) and $Cl^-/(Cl^- + HCO_3^-)$ (0.5–1), located in the lower right corner and reflecting the influence of precipitation;

b) medium TDS (70 to 300 $mg \cdot L^{-1}$) concentrations and low ratios of Na/(Na+Ca) and $Cl^-/(Cl^- + HCO_3^-)$ (<0.5), located in the left side of center and demonstrating the predominance of rock weathering; and

c) high TDS (>300 $mg \cdot L^{-1}$) concentrations and high ratios of Na/(Na+ Ca) and $Cl^-/(Cl^- + HCO_3^-)$ (0.5–1), located in the upper right corner and indicating the dominancy of evaporite dissolution (Gibbs, 1970; Jiang et al., 2015; Stallard and Edmond,1987).

The chemical weathering (calcite, dolomite, Ca, Na-feldspar) and the evaporite dissolution (halite, anhydrite and gypsum) yield different combinations of dissolved ions which play vital role in controlling the hydrogeochemistry of river water. The weathering of carbonates generates Ca, Mg, and HCO_3^-, weathering of silicates generates Ca, Mg, Na, and HCO_3^- and dissolution of evaporites generates Ca, Mg, Na, SO_4^{2-}, and Cl^-. In other words, Ca and Mg primarily originate from the weathering of carbonates, silicates and evaporites, Na and K from the dissolution of evaporites and the weathering of silicates and $SO_4^{2-}$and Cl^- from the evaporites dissolution. With respect to the anions, HCO_3^- is predominantly derived from the weathering of carbonate and silicates minerals, whereas Cl^- and SO_4^{2-} are mainly derived from the halite, sulfide oxidation and soft sulphate minerals such as gypsum (Galy and France-Lanord, 1999; Mortatti and Probst, 2003; Thomas et al., 2015).

Table 3. Ionic ratios of various hydrogeochemical attributes

Location	Ca/Na	Mg/Na	HCO_3^-/Na	HCO_3^-/Ca	Ca/SO_4^{2-}	Na/Cl	HCO_3^-/(HCO_3^-+SO_4^{2-})	Ca+Mg/Tz^+
A1	1.86	0.23	4.75	2.55	2.45	0.62	0.86	0.68
A2	1.70	0.20	5.14	3.02	3.08	0.89	0.90	0.66
A3	1.86	0.23	5.04	2.78	2.11	0.94	0.85	0.67
A4	1.96	0.24	4.95	2.53	2.48	0.88	0.86	0.69
A5	2.51	0.24	5.35	2.13	3.47	0.85	0.88	0.73
A6	1.94	0.17	4.30	2.22	2.75	0.84	0.86	0.68
A7	1.95	0.17	4.09	2.22	2.50	0.36	0.84	0.68
A8	2.32	0.12	2.45	1.05	4.99	0.23	0.84	0.71
A9	2.37	0.12	2.88	1.22	4.42	0.23	0.84	0.71
A10	2.36	0.12	2.36	1.00	3.41	0.22	0.77	0.71
A11	2.27	0.14	2.99	1.32	3.00	0.24	0.80	0.71
A12	2.58	0.47	5.46	2.12	2.58	0.66	0.85	0.75
A13	2.28	0.25	3.71	1.63	2.25	0.31	0.79	0.72
A14	2.32	0.30	3.22	2.10	3.01	0.57	0.86	0.72
A15	1.86	0.18	3.22	1.73	2.01	0.34	0.78	0.67
A16	1.25	0.13	2.23	1.77	1.72	0.44	0.75	0.58
A17	1.40	0.14	2.45	1.75	1.73	0.44	0.75	0.61
A18	2.35	0.16	3.82	1.62	2.36	0.31	0.79	0.72
A19	1.59	0.12	2.55	1.60	2.25	0.37	0.78	0.63
A20	2.34	0.20	2.82	1.20	2.33	0.29	0.74	0.72
A21	2.17	0.12	2.87	1.33	2.66	0.26	0.78	0.70
A22	2.34	0.18	2.94	1.26	2.38	0.24	0.75	0.72

Values expressed as mean, all ratios derived from µeq ratios from µmolar concentrations, Tz+: sum of total cations in µeq

Represented in the Gibbs diagram (Fig. 3), the water samples collected from the selected sampling locations illustrate the dominancy of geogenic factors in the Olt River. However, most of the water samples were characterized by relatively higher concentrations of TDS and wide ranges of Na/(Na+Ca) and Cl^-/(Cl^-+HCO_3^-) ratios, highlighting the major role of evaporation-crystallization processes as a major controlling factor in hydrogeochemistry.

3.4. Principal component analysis

For pattern recognition, Principal Component Analysis (PCA) is a powerful technique that attempts to explain the variance of a large set of intercorrelated variables. It indicates association between variables, thus, reducing the dimensionality of the dataset. PCA extracts the eigen values and eigenvectors from the covariance matrix of original variables. The eigen values of the PCs are the measure of their associated variance, the participation of the original variables in the PCs is given by the loadings, and the individual transformed observations are called scores (Helena et al., 2000; Wunderlin et al., 2001; Singh et al., 2004).

The varimax rotation technique prevents multiple variables from being loaded to a single component, allowing for easy interpretation of significant variables. The varimax factor values which are greater than 0.75 (> 0.75) is considered as "strong", the values range from 0.50-0.75 (0.50 ≥ factor loading ≥ 0.75) is considered as "moderate", and the values range from 0.30-0.49 (0.30 ≥ factor loading ≥ 0.49) is considered as "weak" factor loadings.

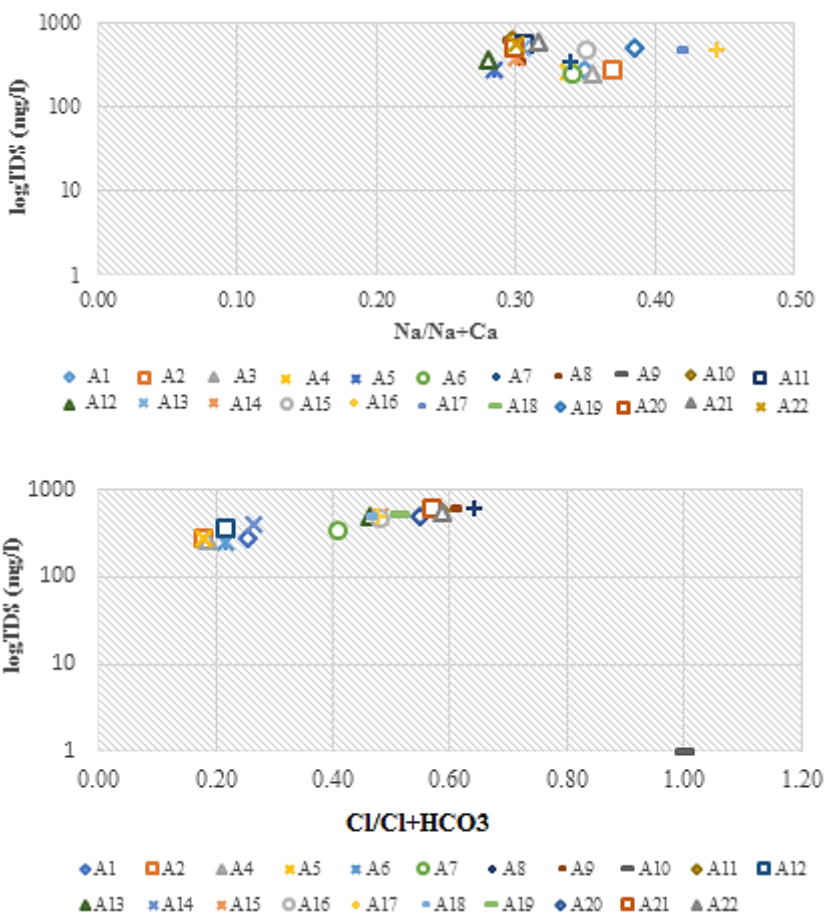

Figure 3. Gibbs plots explain the chemistry and geochemical processes in water samples of the study area

Table 4 summarizes the PCA results including the loadings, eigen values and variance elucidated by each principal component (PCs). The PCA result consists of four PCs that cumulatively account for 77.96% of the total variance in the hydrochemistry. The first component, PC1, which normally accounts for the most significant process, explains 54.86%

of the total variance with an eigenvalue of 5.682. The PC consists of all the major ions, which consists of a moderate positive loading of HCO_3^- and Mg. PC2 accounts for 23.49% of the variance with an eigenvalue of 2.114, which consists of a moderate positive loading of HCO_3^- and Mg.

The loadings plot (Fig.4.) of the first two PCs (PC1 and PC2) shows the distribution of all the physico-chemical parameters in the first (upper right) and fourth (lower right) quadrants. The lines joining the variables and passing through the origin in the plot of the factor loadings are indicative of the contribution of the variables to the samples. Grouping of parameters (Mg, Ca, Na and SO_4^{2-}; EC, TDS, pH, and Cl^-) in the loadings plot suggests their significant mutual positive correlation.

Table 4. Loadings of experimental variables on principal components, Eigen values and variances

Variable	Principal components	
	PC1	*PC2*
pH	0.210	-0.168
$N\text{-}NO_3^-$	-0.280	-0.381
TDS	**0.407**	-0.073
Cl^-	**0.396**	-0.170
SO_4^{2-}	**0.317**	0.189
HCO_3^-	-0.065	**0.611**
EC	**0.404**	-0.076
Ca	**0.385**	0.042
Mg	0.030	**0.613**
Na	**0.371**	0.006
Eigen value	5.682	2.114
Percentage of Variance (%)	54.86	23.49
Cumulative (%)	56.82	77.96

Figure 5 shows mixed distribution of samples. The visible grouping of most of the samples was observed in the left quadrilateral, in the lower part, and in the right quadrants.

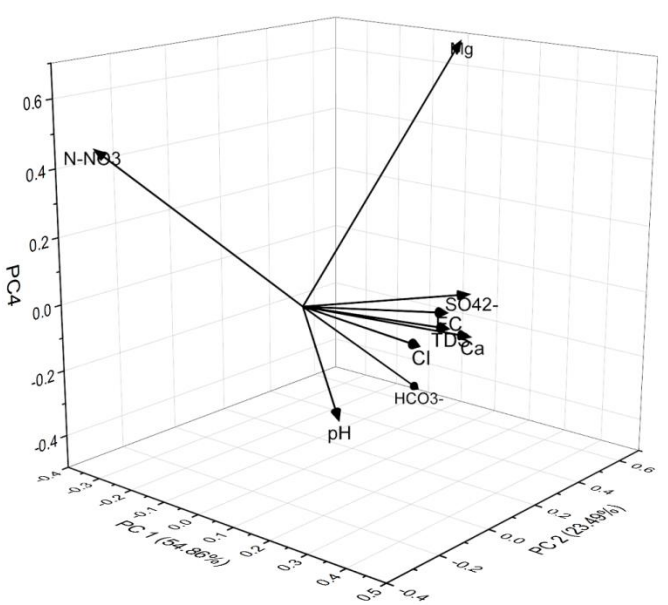

Figure 4. Plots of PCA loadings scores for dataset of water sample

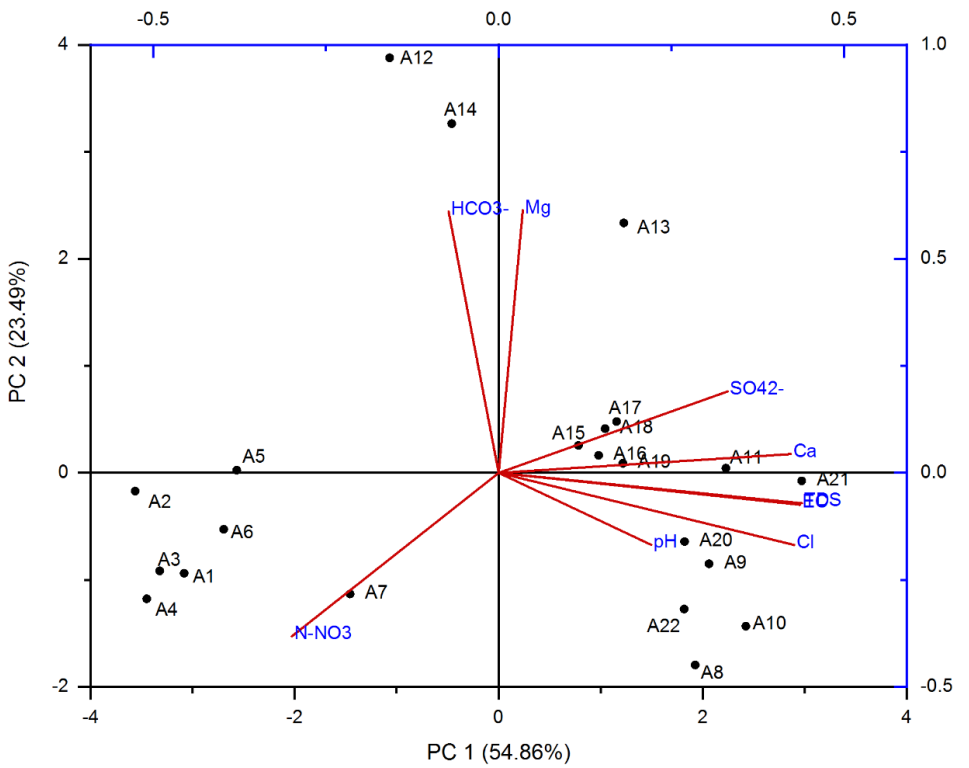

Figure 5. PCs score plot for datasets of water samples

4. CONCLUSION

The hydrogeochemical analysis of Olt River waters reveals that major ion constituents were of the following order: $HCO_3^- > Cl^- > SO_4^{2-} > NO_3^-$ and $Ca^{2+} > Na^+ > Mg^{2+}$. The Piper trilinear diagram was used to illustrate the similarities and differences in the composition of waters and to classify them in to certain chemical types. According to this diagram, the dominant hydrochemical facies in the study area is Ca–Na–HCO_3^-–Cl^-, which represents 87% of the samples. The study area is influenced by natural processes of water–rock interaction such as dissolution of evaporitic rocks (gypsum, anhydrite, and halite).

Gibbs plot, and mixing diagram inferred that the primary mechanism controlling the hydrochemistry of the basin is rock weathering followed by evapo-crystalization. These findings were also confirmed by the relatively high ratios of Ca/Na, HCO_3^-/Na, HCO_3^-/Ca and Ca/SO_4^{2-}.

Acknowledgments: This work is part of the project PN 19110303 “Advanced techniques for identifying sources of contamination and biochemical reactions in aquatic ecosystems” financed by the Ministry of Education and Research, Romania.

Funding: Project PN 19110303, Contract no. 9N/2019, financed by the Ministry of Education and Research, Romania.

Author Contributions: Claudia Sandru set the concept of the paper, draw the draft manuscript and interpreted data; Mihaela Iordache performed the measurement; Andreea Maria Radulescu and

Ramona Ionela Zgavarogea participated at data interpretation; Roxana Elena Ionete revise the data interpretation and graphics and completed the final manuscript.

Conflict of Interest Statement: There is no conflict of interest on this article.

REFERENCES

Forel, F.A. (1892). *Le Léman: monographie limnologique*, Lausanne: F. Rouge.

Galy, A. and France-Lanord, C. (1999). Processes of the weathering in the Ganges-Brahmaputra basin and the riverine alkalinity budget, *Chemical Geology*, *159*, pp. 31-60.

Gibbs, R.J. (1970). Mechanisms controlling world water chemistry, *Science*, 170, pp. 1088-1090.

Helena, B, Pardo, R, Vega, M, Barrado, E, Fernandez, J.M., Fernandez, L. (2000). Temporal evolution of groundwater composition in an alluvial aquifer (Pisuerga River, Spain) by principal component analysis, *Water Res. 34*, pp. 807-816.

Jiang, L., Yao, Z., Liu, Z., Wang, R., Wu, S. (2015). Hydrochemistry and its controlling factors of rivers in the source region of the Yangtze River on the Tibetan Plateau, *Journal Geochem. Explor. 155*, pp. 76-83.

Meybeck, M., Ragu, A. (1995). *River Discharges to the Oceans: An Assessment of Suspended Solids, Major Ions and Nutrients*. UNEP

Meybeck, M. (1982). Carbon, nitrogen, and phosphorus transport by world rivers, *American Journal of Science 282*(4), pp. 401-450.

Mortatti, J., Probst, J.L. (2003). Silicate rock weathering and atmospheric/soil CO_2 uptake in the Amazon Basin estimated from river water geochemistry: seasonal and spatial variations, *Chem. Geol. 197*, pp. 177-196.

Singh KP, Malik A, Mohan D, Sinha S. (2004). Multivariate statistical techniques for the evaluation of spatial and temporal variations in water quality of Gomti River (India)—a case study, *Water Res. 38*, pp. 3980-3992.

SR EN ISO 5667-6, (2017). *Water quality — Sampling —* Part 6: Guidance on sampling of rivers and streams

Stallard, R.F. and Edmond, J.M. (1987). Geochemistry of the Amazon: Weathering chemistry and limits to dissolved inputs, *Journal Geophys. Res., 92*, pp. 8293-8302.

Thomas, J., Joseph, S., Thrivikramji, K.P. (2015). Hydrogeochemical drivers and pro-cesses controlling solute chemistry of two mountain river basins of contrasting climates in the southern Western Ghats, India, In: Ramkumar, Mu, Kumaraswamy, K., Mohanraj, R. (Eds.), *Environmental Management of River Basin Ecosystems*, Springer-Verlag, Heidelberg, pp. 355-396

Zaporozec, A. (1972). Graphical interpretation of water quality data, *Groundwater 10*(2), pp. 32-43.

Wunderlin, D.A., Diaz, M.D.P., Ame, M.V., Pesce, S.F., Hued, A.C., Bistoni, M.D. (2001). Pattern recognition techniques for the evaluation of spatial and temporal variations in water quality. A case study: Suquia River Basin (Cordoba Argentina), *Water Res., 35*, pp. 2881-2894.